

Luteolin Promotes Degradation in Signal Transducer and Activator of Transcription 3 in Human Hepatoma Cells: An Implication for the Antitumor Potential of Flavonoids

Karuppaiyah Selvendiran,¹ Hironori Koga,^{1,2} Takato Ueno,^{1,2} Takafumi Yoshida,^{1,2} Michiko Maeyama,^{1,2} Takuji Torimura,^{1,2} Hirohisa Yano,³ Masamichi Kojiro,³ and Michio Sata^{1,2}

¹Research Center for Innovative Cancer Therapy, and Center of the 21st Century Center of Excellence Program for Medical Science, Kurume University; and ²Second Department of Medicine and ³Department of Pathology, Kurume University School of Medicine, Kurume, Japan

Abstract

In this study, we have investigated the underlying molecular mechanism for the potent proapoptotic effect of luteolin on human hepatoma cells both *in vitro* and *in vivo*, focusing on the signal transducer and activator of transcription 3 (STAT3)/Fas signaling. A clear apoptosis was found in the luteolin-treated HLF hepatoma cells in a time- and dosage-dependent manner. In concert with the caspase-8 activation by luteolin, an enhanced expression in functional Fas/CD95 was identified. Consistent with the increased Fas/CD95 expression, a drastic decrease in the Tyr⁷⁰⁵ phosphorylation of STAT3, a known negative regulator of Fas/CD95 transcription, was found within 20 minutes in the luteolin-treated cells, leading to down-regulation in the target gene products of STAT3, such as cyclin D1, survivin, Bcl-xL, and vascular endothelial growth factor. Of interest, the rapid down-regulation in STAT3 was consistent with an accelerated ubiquitin-dependent degradation in the Tyr⁷⁰⁵-phosphorylated STAT3, but not the Ser⁷²⁷-phosphorylated one, another regulator of STAT3 activity. The expression level of Ser⁷²⁷-phosphorylated STAT3 was gradually decreased by the luteolin treatment, followed by a fast and clear down-regulation in the active forms of CDK5, which can phosphorylate STAT3 at Ser⁷²⁷. An overexpression in STAT3 led to resistance to luteolin, suggesting that STAT3 was a critical target of luteolin. In nude mice with xenografted tumors using HAK-1B hepatoma cells, luteolin significantly inhibited the growth of the tumors in a dosage-dependent manner. These data suggested that luteolin targeted STAT3 through dual pathways—the ubiquitin-dependent degradation in Tyr⁷⁰⁵-phosphorylated STAT3 and the gradual down-regulation in Ser⁷²⁷-phosphorylated STAT3 through inactivation of CDK5, thereby triggering apoptosis via up-regulation in Fas/CD95. (Cancer Res 2006; 66(9): 4826-34)

Introduction

Flavonoids are polyphenolic compounds occurring naturally in the plant kingdom, displaying a wide range of pharmacologic properties, including anti-inflammatory, anticarcinogenic, and

anticancer effects (1). Luteolin, the flavone subclass of flavonoids, usually occurs in its glycosylated form in celery, green pepper, perilla leaf, and camomile tea, etc., and much as an aglycone in perilla seeds. Recently, a potent anticancer effect of luteolin has been shown in several experiments *in vitro*; however, the bioavailability of luteolin has not yet been fully tested. Only one study on mouse skin cancer development has shown an anticancer effect of the luteolin-containing perilla leaf extract *in vivo* (2), suggesting a potential anticancer effect of any form of luteolin *in vivo*.

Apoptosis is supposed to be the main mechanism of the anticancer effects of luteolin, although other mechanisms, such as cell cycle inhibition by inactivating cyclin-dependent kinase 2 (CDK2; ref. 3), and antiangiogenesis by inhibiting vascular endothelial growth factor (VEGF)-induced phosphatidylinositol 3'-kinase activity (4), have been shown. The suggested mechanisms for the luteolin-induced apoptosis include activation of wild-type p53 (5), inactivation of receptor tyrosine kinase (6, 7), inactivation of topoisomerases (8, 9), sensitization to tumor necrosis factor- α (TNF- α ; ref. 10), imbalance in Bcl-2 family of proteins (11–13), and inhibition of fatty acid synthase activity (14).

Signal transducer and activator of transcription 3 (STAT3) is a key signaling molecule for many cytokines and growth factor receptors (15). In addition, STAT3 is constitutively activated in a number of human tumors and possesses oncogenic potential and antiapoptotic activities (16–18). STAT3 is activated by phosphorylation at the Tyr⁷⁰⁵ residue, which induces dimerization, nuclear translocation, and DNA binding (19). Transcriptional activation seems to also be regulated by phosphorylation at the Ser⁷²⁷ residue, apparently via mitogen-activated protein kinase or via a mammalian target of rapamycin pathways (20, 21). Recently, the oncogenic transcription factor STAT3 has attracted much attention as a pharmacologic target, although *in vivo* evidence suggesting that inhibiting STAT3 could counteract cancer has remained incomplete (22).

CDK5 plays an essential role in both the development of the central nervous system during mammalian embryogenesis and maintenance of the neuronal architecture in the adult. Its deregulation has been implicated in neurodegenerative diseases (23). Although CDK5 binds to cyclins D and E, the activation of CDK5 requires one of its regulatory subunits, p35 or p39 (23). The extraneuronal expression of CDK5/p35 has been identified (24); however, the functional roles of CDK5 in the extraneuronal cells, such as liver cancer cells, have not yet been fully examined. Recently, CDK5 has been shown to regulate the phosphorylation of STAT3 on the Ser⁷²⁷ residue (25), suggesting that CDK5

Requests for reprints: Hironori Koga, Second Department of Medicine, Kurume University School of Medicine, 67 Asahi-machi, Kurume 830-0011, Japan. Phone: 81-942-31-7561; Fax: 81-942-34-2623; E-mail: hirokoga@med.kurume-u.ac.jp.

©2006 American Association for Cancer Research.
doi:10.1158/0008-5472.CAN-05-4062

participated in the oncogenic process through regulation of the STAT3 activity in neoplastic cells.

The aims of the present study were to clarify the detailed apoptotic mechanism of luteolin in human hepatoma cells *in vitro* and to assess the antitumor potential of luteolin *in vivo*. Here, we show a novel mechanism for luteolin-induced apoptosis to promote Tyr⁷⁰⁵-phosphorylated STAT3 degradation. This unique mechanism of luteolin may lay the basis for the potent anticancer effect of luteolin, because STAT3 regulates expressions of crucial tumor-promoting gene products, including cyclin D1, survivin, Bcl-xL, and VEGF. We also show the luteolin-induced activation of Fas/CD95-mediated apoptosis through attenuation in the STAT3 expression. The *in vivo* antitumor effect of luteolin against hepatoma cell xenografts in nude mice suggests the bioavailability of this flavonoid.

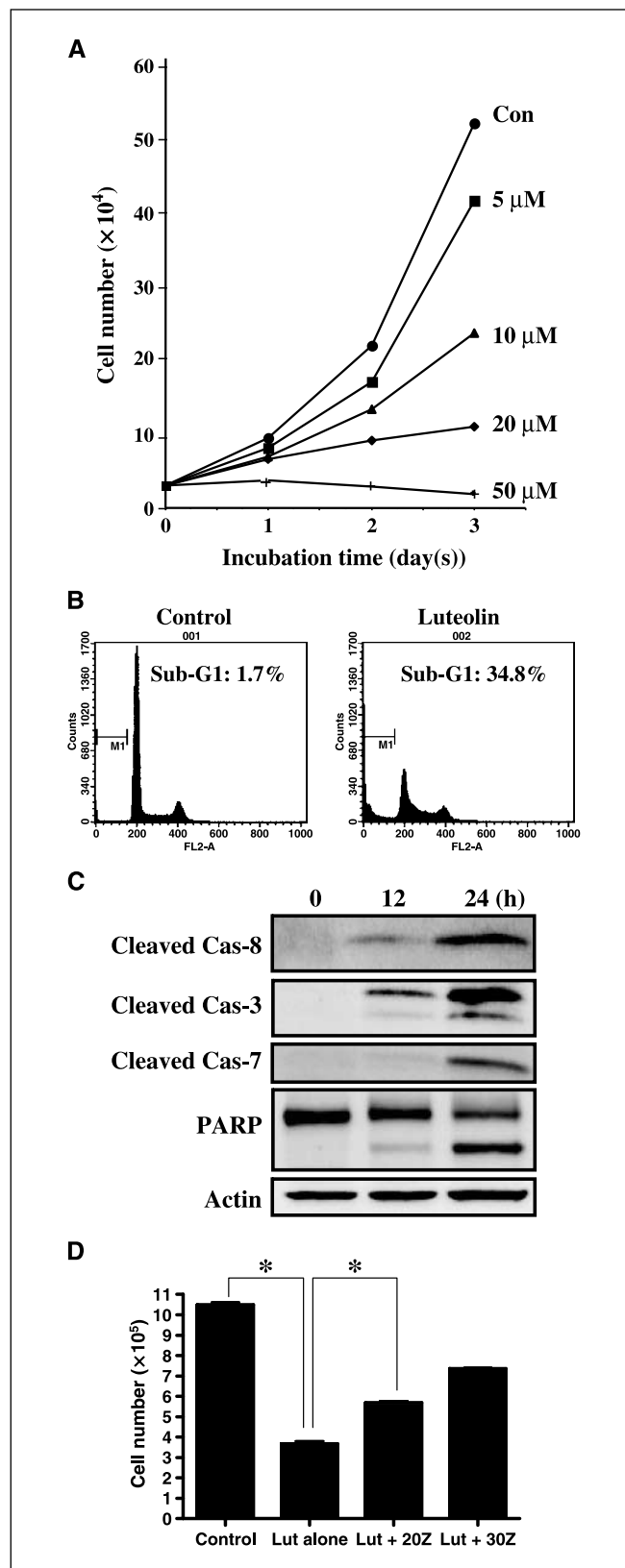
Materials and Methods

Materials. Luteolin was isolated from perilla seeds and purified using high-performance liquid chromatography (purity >95%; Oryza Oil and Fat Chemical, Ichinomiya, Japan). Apigenin and (–)-epigallocatechin-3-gallate were purchased from Wako Pure Chemical Industries (Osaka, Japan). Recombinant human IFN- γ and recombinant human interleukin (IL)-6 were obtained from PeproTech (Rocky Hill, NJ). Antibodies against poly(ADP)ribose polymerase (PARP); Bcl-xL; survivin; phosphorylated STAT1; Tyr⁷⁰⁵-phosphorylated STAT3; caspase-3; and cleaved caspase-3, caspase-7, and caspase-8 were purchased from Cell Signaling Technology (Beverly, MA). Anti-Fas/CD95 antibodies were from BD Biosciences (Franklin Lakes, NJ; clone DX2), and MBL (Nagoya, Japan; clone CH-11), respectively. Antibodies against glyceraldehyde-3-phosphate dehydrogenase (GAPDH), TNF receptor 1 (TNFR1), Fas/CD95 ligand, STAT1, STAT3, Ser⁷²⁷-phosphorylated STAT3, STAT5, VEGF, ubiquitin, cyclin D1, CDK5, Tyr-phosphorylated CDK5, Ser-phosphorylated CDK5, and p35 were from Santa Cruz Biotechnology (Santa Cruz, CA). Antibodies against actin and FLAG were from Sigma (St. Louis, Missouri). MG-132, ALLN, roscovitine, and Ubiquitinated Protein Enrichment kit were from Calbiochem (San Diego, CA), and recombinant protein G agarose and the Lipofectamine kit were from Invitrogen (Carlsbad, CA). The caspase inhibitor Z-VAD-FMK was from Promega Corporation (Madison, WI). Enhanced chemiluminescence (ECL) reagents were obtained from Amersham Pharmacia Biotech (Buckinghamshire, United Kingdom), and the protein assay reagents were from Bio-Rad (Hercules, CA). The RNeasy kit was purchased from Qiagen (Valencia, CA). All other reagents and compounds were analytic grades.

Cell lines and cultures. Three human hepatoma cell lines, HepG2, HLF, and HAK-1B, and the human neuroblastoma cell line IMR-32 were used in this study. HepG2 and HLF were obtained from the Cancer Cell Repository of Tohoku University (Sendai, Japan) and the Human Science Research Resources Bank (Sennan, Japan), respectively. IMR-32 was from RIKEN BioResource Center (Tsukuba, Japan). HAK-1B was established in the

Department of Pathology at our university (26). This cell line was well characterized and has often been used for s.c. transplantation into nude mice (27). Each cell line was grown in DMEM (Sigma-Aldrich Japan, Tokyo, Japan) supplemented with 10% heat-inactivated (56C, 30 minutes) fetal

Figure 1. The proliferation-inhibitory effect of luteolin on HLF hepatoma cells. **A**, 2×10^4 HLF cells were seeded on a 60-mm-diameter dish, and incubated with each concentration of luteolin indicated up to 3 days. The cell number was counted at days 1, 2, and 3 after the seeding. Both a dosage- and a time-dependent inhibition of cell proliferation are shown. **B**, HLF cells were subjected to the 50 $\mu\text{mol/L}$ luteolin treatment for 48 hours (control, vehicle-treated). Cells were then harvested, and the sub-G₁ population for 50,000 events within a fixed gate was analyzed. The indicated percentages are the mean of three independent experiments, each in duplicate. **C**, each sample of cell lysate containing of 50 μg protein was subjected to the immunoblot analysis for apoptosis. Cleavages in caspase-8, caspase-3, caspase-7, and PARP are clearly shown in the 50 $\mu\text{mol/L}$ luteolin-treated HLF cells. **D**, 3×10^5 cells were seeded onto a 35-mm-diameter dish and cultured for 24 hours. Z-VAD-FMK or the vehicle (DMSO) was added to the medium at 1 hour before the 50 $\mu\text{mol/L}$ luteolin treatment. After the 48-hour incubation, the attached cells were counted. *, $P < 0.001$; Lut, luteolin; 20Z, 20 $\mu\text{mol/L}$ Z-VAD-FMK; 30Z, 30 $\mu\text{mol/L}$ Z-VAD-FMK.



bovine serum (BioWest, Nuail, France), 100 units/mL penicillin, and 100 µg/mL streptomycin (Invitrogen) in a humidified atmosphere of 5% CO₂ at 37°C.

Cell counting. The cell numbers of both untreated and luteolin-treated HLF cells were counted using a CDA-500 automated cell counter (Sysmex, Kobe, Japan).

Cell cycle analysis by flow cytometry. The DNA content was assessed by staining ethanol-fixed cells with propidium iodide and monitoring by FACSCalibur (Becton Dickinson, Franklin Lakes, NJ). The percentage of cells in the sub-G₁ apoptotic cell population was determined using CELLQuest software (Becton Dickinson).

Immunoblot analysis. Hepatoma cells were lysed in lysis buffer [50 mmol/L Tris-HCl (pH 8.0), 150 mmol/L NaCl, 0.5% NP40, 1 mmol/L EDTA (pH 8.0), 1 mmol/L EGTA (pH 8.0), 0.1 mmol/L sodium fluoride (NaF), 0.1 mmol/L sodium orthovanadate (Na₃VO₄), 1 mmol/L DTT, 2 µg/mL aprotinin, and 2 µg/mL leupeptin]. Cell lysates were centrifuged at 12,000 × *g* for 20 minutes at 4°C, and the supernatant was separated. Xenografted tumor tissue samples were homogenized on ice in the lysis buffer, and the homogenate was clarified by centrifugation. The protein concentration was measured using a Bio-Rad protein assay kit. After being boiled for 5 minutes in the presence of 2-mercaptoethanol, samples containing cell or tissue lysate protein were separated on 10% or 15% SDS-polyacrylamide gel and then transferred onto equilibrated polyvinylidene difluoride membranes (Bio-Rad). After skimmed milk blocking, the membranes were incubated with the primary antibodies described above. The bound antibodies were detected with horseradish peroxidase (HRP)-labeled sheep anti-mouse IgG or HRP-labeled donkey anti-rabbit IgG (Amersham Pharmacia Biotech) using the enhanced chemiluminescence detection system (ECL Advanced kit). A positive signal from the target proteins was visualized using an image analyzer LAS-1000 plus (Fujifilm, Tokyo, Japan), and the fold increase and percentage reduction in the protein expressions were determined using an Image Gauge version 3.45 (Fujifilm).

Immunofluorescence confocal laser scanning microscopy. Immunocytochemistry was done as previously reported (28). Hepatoma cells, grown on Lab-Tek Chamber Slides (Nalge Nunc Int, Naperville, IL), were fixed with 4% paraformaldehyde for 10 minutes at room temperature, and then washed in PBS containing 0.05% Tween 20 (PBS-T). Nonspecific reactions were blocked with protein block serum-free (DAKO Japan, Kyoto, Japan) and then incubated with an anti-Tyr⁷⁰⁵-phosphorylated STAT3 antibody at 4°C overnight. After washing in PBS-T, the specimens were treated with Alexa Fluor goat anti-mouse IgG (H+L) antibody (Molecular Probes, Eugene, OR) for 30 minutes at room temperature, and then counterstained by propidium iodide after digestion of RNA by RNase (Nippon Gene, Tokyo, Japan). A confocal laser scanning microscope (FLUOVIEW FV300; Olympus, Tokyo, Japan) equipped with an argon/krypton laser capable of dual excitation and detection was used to visualize the immunostaining for Tyr⁷⁰⁵-phosphorylated STAT3 protein and the nuclear localization of propidium iodide. The negative stain control was done by omitting the primary antibody in the above experiment.

Reverse transcription-PCR. Total RNA was isolated from HLF cells using the RNeasy system according to the instructions of the manufacturer. RNA quantification was done using spectrophotometry. Reverse transcription-PCR (RT-PCR) analysis for the mRNA expressions in Fas/CD95 and the internal control GAPDH was carried out using a GeneAmp PCR System 9700 (Applied Biosystems, Foster City, CA), under the following conditions: initial denaturation at 94°C for 2 minutes, 35 cycles of amplification (denaturation at 94°C for 30 seconds, annealing at 50°C for 30 seconds, and extension at 72°C for 30 seconds), and extension at 72°C for 5 minutes. The sequences (5'-3') for the primer pairs of Fas/CD95 and GAPDH, respectively, were as follows: Fas/CD95, CAAGGGATTGAAATTGAGGA (forward) and GACAAAGCCACCCAAGTTA (reverse); GAPDH, GTCAACGGATTTGGTCGTATT (forward) and AGTCTTCTGGGTGGCAGTGAT (reverse). The PCR products were electrophoresed on 1.5% agarose gel, and stained with ethidium bromide.

Transfection of wild-type STAT3 cDNA. The STAT3 overexpression experiments were done using a wild-type STAT3 cDNA as previously described (29). The FLAG-tagged gene was transfected into HLF cells using the Lipofetamine kit according to the protocol of the manufacturer. At

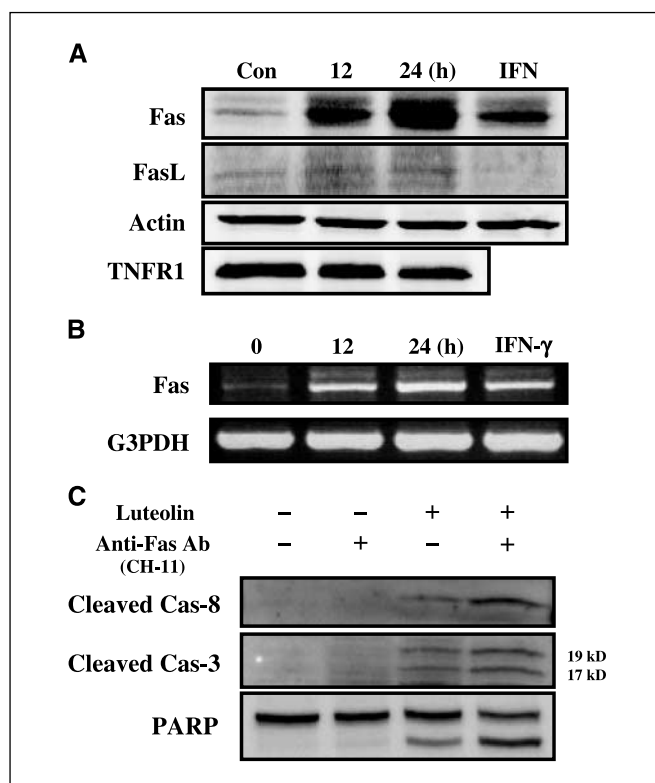


Figure 2. A, immunoblot analysis for the expression levels of caspase-8-associated death receptors, such as Fas/CD95 and TNFR1, and Fas/CD95 ligand (*FasL*). A clear increase in the Fas/CD95 expression, but not in the TNFR1 expression, is detected in the 50 µmol/L luteolin-treated HLF cells. The expression level of Fas/CD95 ligand is low and unchanged. B, the expression level of Fas/CD95 mRNA is increased in the 50 µmol/L luteolin-treated hepatoma cells. The IFN-γ (100 units/mL)-induced Fas/CD95 mRNA expression was set as a positive control. C, after incubation with 50 µmol/L luteolin for 12 hours, the agonistic anti-Fas/CD95 antibody (clone CH-11; dilution, 1:5,000) was added into the culture medium for the hepatoma cells. After treatment with the antibody for 4 hours, the cells were then prepared for immunoblot analyses of cleaved caspase-8, cleaved caspase-3, and PARP. The agonistic anti-Fas/CD95 antibody clearly increases the cleavages in caspase-8, caspase-3, and PARP, suggesting the enhanced apoptosis through stimulation of the newly synthesized Fas/CD95.

24 hours after the transfection of the *STAT3* gene, luteolin (50 µmol/L) was added into the culture medium of the cells, and the cells were subjected to immunoblots for Tyr⁷⁰⁵-phosphorylated STAT3, total STAT3, cleaved caspase-3, PARP, and FLAG. The untransfected cells without the luteolin exposure, the untransfected cells with the luteolin exposure, the Lipofetamine-treated cell with the luteolin exposure, and the empty vector-transfected cells with the luteolin exposure were set as the controls.

Ubiquitination assay and immunoprecipitation. For the enrichment of any ubiquitinated proteins, affinity matrices consisting of a glutathione *S*-transferase fusion protein containing the ubiquitin-associated domains of Rad23 conjugated to glutathione-agarose (Ubiquitinated Protein Enrichment kit) were used. The affinity matrices were incubated with untreated or luteolin-treated HLF cell extracts (500 µg protein) in the lysis buffer for 2 hours. Then, the matrices were washed four times with the same buffer, and bound proteins were eluted with SDS loading buffer. The ubiquitinated protein-enriched samples were subjected to immunoblotting for ubiquitin, STAT3, Ser⁷²⁷-phosphorylated STAT3, and Tyr⁷⁰⁵-phosphorylated STAT3. Visualized smear signals were estimated as the polyubiquitinated target proteins. Immunoprecipitation was done as previously described (30) using an anti-STAT3 antibody for HLF cell lysates containing 200 µg protein.

Effects of luteolin on xenografted tumor growth in nude mice. Cultured HAK-1B (10⁷ per mouse) was s.c. injected into the back of 5-week-old male BALB/c athymic nude mice (Clea Japan, Osaka, Japan). At 5 to

7 days later when the largest diameter of the tumor had reached ~5 to 8 mm, the mice were divided into three groups ($n = 10$ each) in a manner to equalize the mean tumor diameter among the three groups. Each mouse was given the CL-2 control diet, 50 or 200 ppm luteolin-containing CL-2-based diet (Clea Japan). The tumor size was measured in two orthogonal directions using calipers weekly, and the tumor volume (mm^3) was estimated using the equation $\text{length} \times (\text{width})^2 \times 0.5$. At 6 weeks after the luteolin feeding, the mice were sacrificed and the tumors were resected. The tumor tissues were subjected to immunoblotting. All animal experiments were conducted in accordance with the NIH Guidelines for the Care and Use of Laboratory Animals and were approved by the University of Kurume Institutional Animal Care and Use Committee.

Statistical analysis. Statistical significance was assessed using Mann-Whitney U test. $P < 0.05$ was considered statistically significant.

Results

Luteolin inhibited cell proliferation, inducing apoptosis.

Luteolin clearly inhibited proliferation in HLF cells in both dosage- and time-dependent manner. A 43.6% reduction in cell number was found in the luteolin-treated cells at a concentration of 10 $\mu\text{mol/L}$ on day 3 (Fig. 1A). An induction in apoptosis contributed to this inhibition in cell proliferation (Fig. 1B). Moreover, 50 $\mu\text{mol/L}$ luteolin showed a clear apoptosis in HLF cells within 12 hours, showing cleavages for caspase-8, caspase-3, caspase-7, and PARP in immunoblotting (Fig. 1C). Consistent with this finding, the caspase inhibitor Z-VAD-FMK significantly inhibited the luteolin-induced apoptosis in a dosage-dependent manner (Fig. 1D).

Involvement of Fas/CD95 in luteolin-induced apoptosis.

Because caspase-8 was activated by luteolin, we examined the expression level of caspase-8-associated death receptors, such as Fas/CD95 and TNFR1. Indeed, a clear increase in Fas/CD95 expression, but not in TNFR1, was found in the luteolin-treated HLF cells (Fig. 2A), suggesting a significant involvement of Fas/CD95 in the luteolin-induced apoptosis. The expression level in the Fas/CD95 ligand in the luteolin-treated cells showed no change in comparison with that in the control cells (Fig. 2A), as recently reported in HepG2 cells (12). To confirm whether the increased expression in Fas/CD95 was due to its transcriptional induction, we did RT-PCR analysis for Fas/CD95 mRNA. The luteolin-treated HLF cells clearly showed an increased expression in Fas/CD95 mRNA (Fig. 2B). Then, we examined whether this up-regulated Fas/CD95 was functional in inducing apoptotic signals. We stimulated the luteolin-treated cells by an apoptosis-

inducing anti-Fas/CD95 antibody (clone CH-11) and found that the pretreated cells became more sensitive to this antibody. This indicated that the newly synthesized Fas/CD95 was functional in mediating the apoptotic signals in the luteolin-treated human hepatoma cells (Fig. 2C).

Decrease in the expression level of phosphorylated STAT3s.

Transcription of *Fas/CD95* is negatively regulated by STAT3, especially by its phosphorylated forms—Tyr⁷⁰⁵-phosphorylated

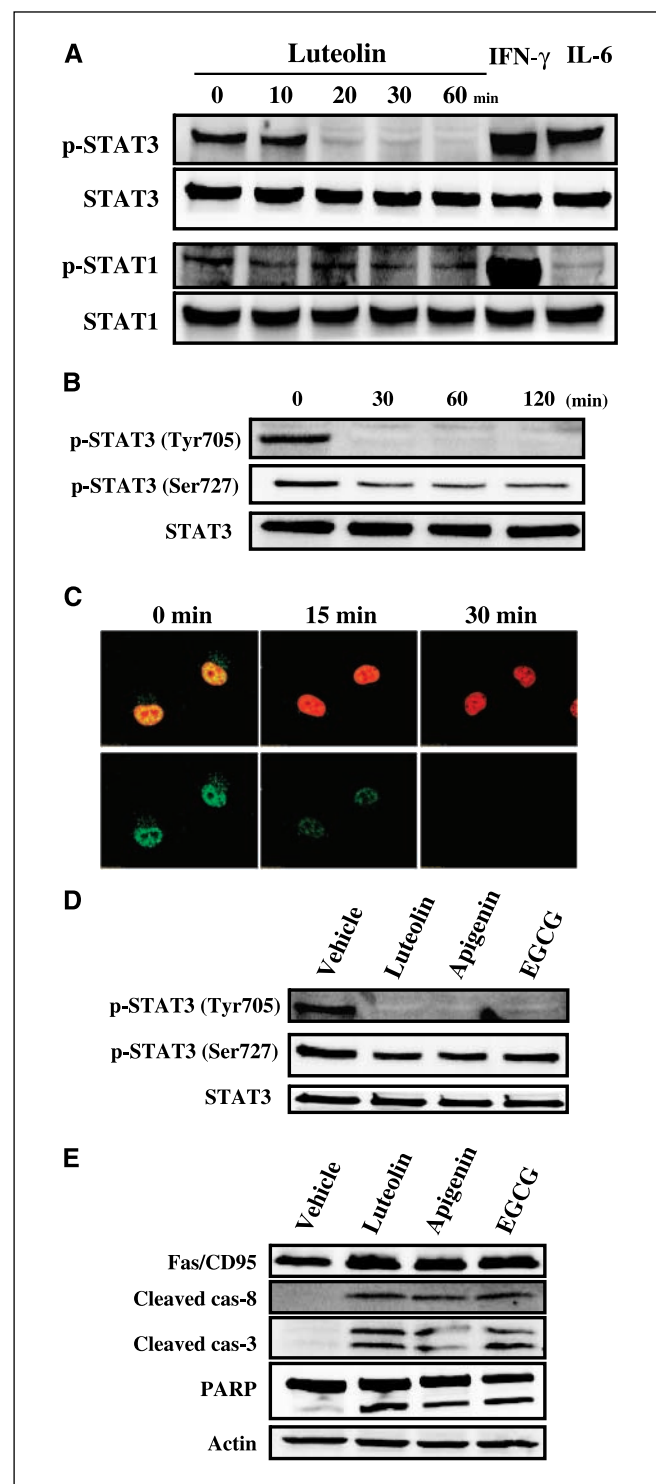


Figure 3. A, the time course study for the expression levels of STAT3 and STAT1 and their phosphorylated counterparts by immunoblot assay. The cells were treated with 50 $\mu\text{mol/L}$ luteolin for 0, 10, 20, 30, and 60 minutes, respectively. For positive controls for Tyr⁷⁰⁵-phosphorylated STAT3 (p-STAT3), HLF cells were incubated with IFN- γ (100 units/mL) and IL-6 (2 ng/mL). As for the positive control for phosphorylated STAT1 (p-STAT1), the IFN- γ -stimulated cells were used. The expression level of Tyr⁷⁰⁵-phosphorylated STAT3 rapidly decreases after the 10-minute treatment of luteolin; however, that of phosphorylated STAT1 is unchanged by the luteolin treatment. B, a gradual decrease in the expression level of Ser⁷²⁷-phosphorylated STAT3 [p-STAT3 (Ser⁷²⁷)] is noted in the luteolin-treated cells, compared with a marked decrease in that of Tyr⁷⁰⁵-phosphorylated one [p-STAT3 (Tyr⁷⁰⁵)]. The total STAT3 expression level is almost unchanged. C, the active Tyr⁷⁰⁵-phosphorylated STAT3 is confirmed to be in the nuclei of the hepatoma cells (green signal), and the expression of this type of STAT3 is diminished to an undetectable level within 30 minutes, which is consistent with the finding in the immunoblot analysis. D, other flavonoids, such as apigenin (25 $\mu\text{mol/L}$) and (-)-epigallocatechin-3-gallate (EGCG, 150 $\mu\text{mol/L}$), also show potential to decrease the expression level of Tyr⁷⁰⁵-phosphorylated STAT3 to an undetectable level at 30 minutes after the treatments. E, the increase in the Fas/CD95 expression and the cleavages in caspase-8, caspase-3, and PARP are noted at 24 hours after the treatments with the flavonoids.

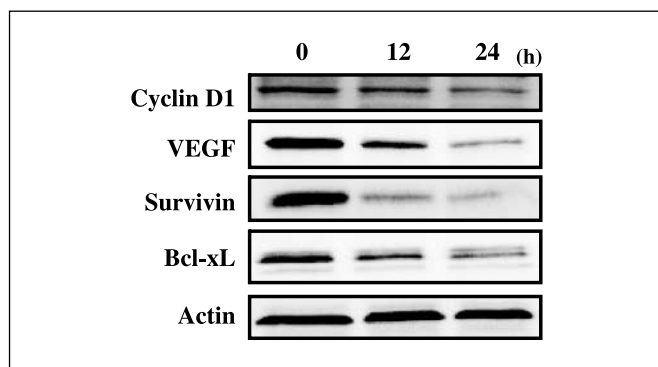


Figure 4. To assess the expression levels in the downstream gene products of STAT3, such as cyclin D1, VEGF, survivin, and Bcl-xL, the immunoblot analysis was done using the HLF cells exposed to 50 $\mu\text{mol/L}$ luteolin for 12 and 24 hours. All of the gene products are found to be decreased in their expression levels by the luteolin treatment.

STAT3 and Ser⁷²⁷-phosphorylated STAT3 (31). Thus, the increase in the expression level of Fas/CD95 by the luteolin treatment in this study encouraged us to investigate a possible decrease in the expression level of the phosphorylated STAT3s. And indeed, the expression level of Tyr⁷⁰⁵-phosphorylated STAT3, a major phosphorylated STAT3, was drastically decreased within 20 minutes, although that of total STAT3 was mostly unchanged (Fig. 3A). In contrast to the rapid decrease in the Tyr⁷⁰⁵-phosphorylated STAT3 expression level, a gradual decrease was found in the expression level of Ser⁷²⁷-phosphorylated STAT3 (Fig. 3B). To ensure that this effect of luteolin was specific on the phosphorylated STAT3s, changes in the expression levels of phosphorylated STAT1 and phosphorylated STAT5 were examined using immunoblot analysis, resulting in no change in the phosphorylated STAT1 expression (Fig. 3A). STAT5 was barely expressed in the hepatoma cells used (data not shown). The drastic decrease in the nuclear Tyr⁷⁰⁵-phosphorylated STAT3 was confirmed by immunocytochemistry using a confocal laser scanning microscope (Fig. 3C). Then, we assessed whether the specific decrease in the expression level of Tyr⁷⁰⁵-phosphorylated STAT3 occurred universally in other flavonoids, including apigenin and (-)-epigallocatechin-3-gallate. These two flavonoids also decreased the expression of Tyr⁷⁰⁵-phosphorylated STAT3 to an undetectable level at an early time point (within 30 minutes after treatment; Fig. 3D), followed by an increased expression of Fas/CD95 and the cleavages in caspase-8, caspase-3, and PARP at 24 hours after treatment (Fig. 3E).

Down-regulation in the STAT3 target genes. Because the oncogenic transcription factor STAT3 hierarchically up-regulates the tumorigenic genes, such as *cyclin D1*, *survivin*, *Bcl-xL*, and *VEGF* (15), we investigated the expression levels of the protein products of these genes by immunoblot assay. Indeed, all the gene products were clearly down-regulated (Fig. 4). Because these genes are involved in cell cycle progression (*cyclin D1*), antiapoptosis (*survivin* and *Bcl-xL*), and angiogenesis (*VEGF*), the down-regulation in these genes suggested a profound antitumor potential of luteolin even *in vivo*.

STAT3 overexpression leads to resistance to luteolin-induced apoptosis. If STAT3 was a critical target of luteolin, a profound expression of STAT3 should attenuate luteolin-induced apoptosis. To assess this hypothesis, we did a STAT3-overexpression experiment using cDNA of wild-type STAT3. The

wild-type STAT3-overexpressing HLF cells showed an increased expression level in total STAT3, also generating a profound expression of both Tyr⁷⁰⁵-phosphorylated STAT3 and Ser⁷²⁷-phosphorylated STAT3. Despite luteolin treatment, the STAT3-overexpressing HLF cells had a clearly detectable level in the expression of Tyr⁷⁰⁵-phosphorylated STAT3, which was fragile against luteolin in our system. As a result, the luteolin-treated STAT3-overexpressing cells showed no enhanced cleavages in caspase-3 or PARP, in

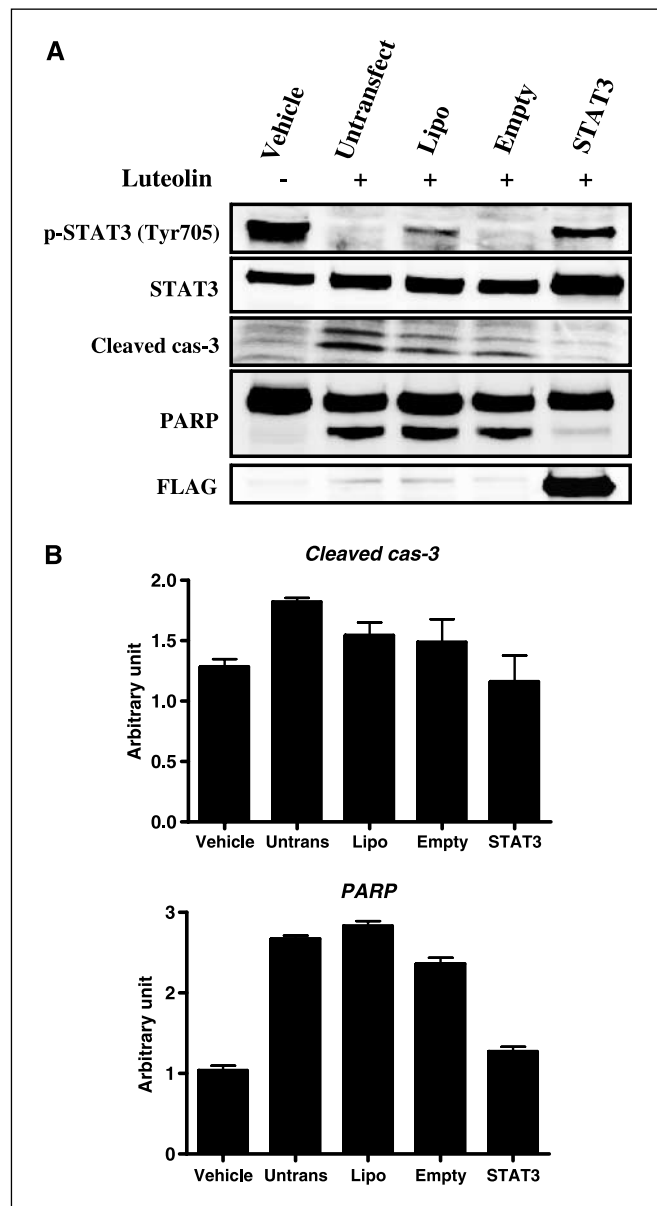


Figure 5. Resistance to the luteolin-induced apoptosis in the STAT3-overexpressing hepatoma cells. **A**, the *STAT3/FLAG* gene was transiently transfected into HLF cells by the lipofection method. At 24 hours after the transfection of the *STAT3* gene, luteolin (50 $\mu\text{mol/L}$) was added into the culture medium of the cells. The untransfected cells with the luteolin exposure (*Untransfect*), the LipofectAMINE-treated cells with the luteolin exposure (*Lipo*), and the empty vector-transfected cells with the luteolin exposure (*Empty*) were set as controls. The *STAT3* gene-transfected HLF cells (*STAT3*) inhibit the luteolin-induced cleavages of both caspase-3 and PARP, showing an increased amount of total STAT3 and the detectable expression levels of Tyr⁷⁰⁵-phosphorylated STAT3 and FLAG. **B**, densitometric analyses of visualized bands for cleaved caspase-3 and PARP. Columns, mean of three independent experiments; bars, SD.

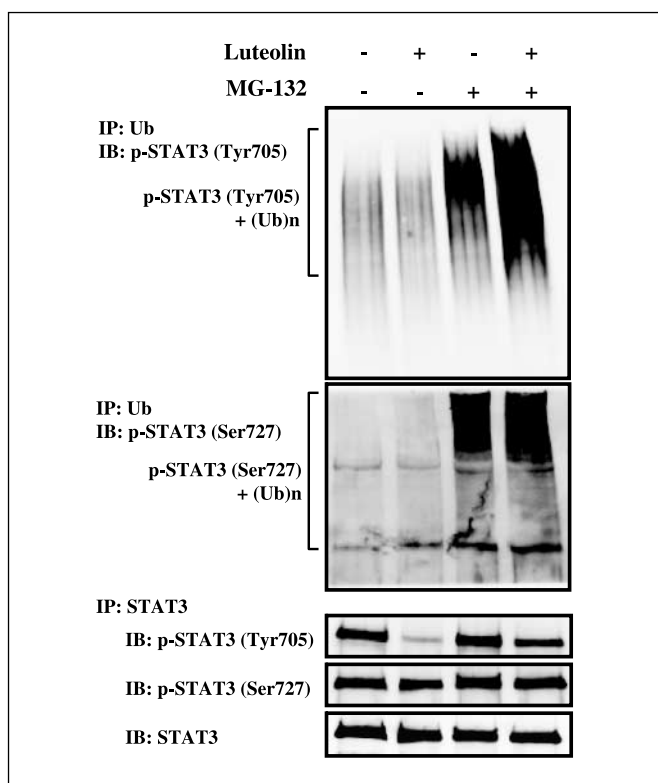


Figure 6. To catch any ubiquitinated proteins in the cell lysates, agarose beads coated with domains having affinity to ubiquitin were incubated in the lysates at 4°C for 2 hours. After washing the beads, the ubiquitinated proteins were subjected to immunoblot for Tyr⁷⁰⁵-phosphorylated STAT3 and Ser⁷²⁷-phosphorylated STAT3. A part of the lysate was also subjected to immunoprecipitation with anti-STAT3 antibody, and the immunoprecipitates were blotted by the antibodies for Tyr⁷⁰⁵-phosphorylated STAT3, Ser⁷²⁷-phosphorylated STAT3, and total STAT3. A predominant ubiquitination of the Tyr⁷⁰⁵-phosphorylated STAT3 is seen in the luteolin-treated cells under proteasomal inhibition using MG-132 (50 μmol/L). In contrast, no clear increase in the ubiquitination of Ser⁷²⁷-phosphorylated STAT3 is found by the luteolin treatment.

comparison with the controls including the empty vector-transfected cells (Fig. 5A and B), suggesting that luteolin might target, at least in part, STAT3 in the hepatoma cells.

Luteolin preferentially promotes ubiquitination of Tyr⁷⁰⁵-phosphorylated STAT3. It is known that the intracellular amount of rapid-turnover proteins, including phosphorylated STAT3, is tightly regulated by the ubiquitin-dependent proteolytic pathway (30, 32, 33). In this study, a fast and marked decrease in the Tyr⁷⁰⁵-phosphorylated STAT3 expression was found in the luteolin-treated cells, encouraging us to investigate any involvement of ubiquitin-dependent degradation in the drastic decrease in Tyr⁷⁰⁵-phosphorylated STAT3 expression. Because HLF cells profoundly expressed the phosphorylated STAT3s, ubiquitination of the endogenous phosphorylated STAT3s was detected using the Ubiquitinated Protein Enrichment kit (Fig. 6). It was noteworthy that an enhanced polyubiquitination on Tyr⁷⁰⁵-phosphorylated STAT3, but not on Ser⁷²⁷-phosphorylated STAT3, was detected in the luteolin-treated cells, under the condition of coincubation with MG-132, a proteasome inhibitor (Fig. 6). This finding strongly suggested that luteolin ubiquitinated STAT3 in a phosphorylation site-specific manner in the human hepatoma cells.

Luteolin suppresses the expression level of tyrosine-phosphorylated CDK5. Recently, it has been shown that STAT3 is

phosphorylated at a Ser⁷²⁷ residue by CDK5, a unique member of the CDK family (25). The activity of CDK5 is regulated by both formation of a complex with the partner molecule p35 (but not cyclins), and Tyr phosphorylation of CDK5 by a putative CDK5 kinase (23). Because we found a gradual decrease in Ser⁷²⁷-phosphorylated STAT3, we investigated any possible earlier decrease in the p35 expression and/or the Tyr-phosphorylated CDK5 expression. To examine these expression levels, we set a positive control using the neuronal cell line, IMR-32, which has been shown to express a profound active CDK5 (34). HLF cells also expressed CDK5; however, its expression level was low in comparison with that of IMR cells. A clear decrease was identified in the expression level of Tyr-phosphorylated CDK5, but not in that of p35, in a luteolin dosage-dependent manner (Fig. 7A), suggesting less involvement of the p35 system in regulating Ser⁷²⁷ phosphorylation of STAT3 in the human hepatoma cells. In the time course experiments, the decrease in the expression level of Tyr-phosphorylated CDK5 was confirmed as an earlier event than the decrease in that of Ser⁷²⁷ phosphorylation of STAT3 (Fig. 7B). These findings suggested that luteolin predominantly decreased the expression level of Tyr-phosphorylated CDK5, thereby decreasing the expression level of Ser⁷²⁷-phosphorylated STAT3, which was, at least in part, responsible for the attenuated activity of STAT3.

Inhibition in xenografted tumor growth by luteolin. Before going to animal experiments, we confirmed the potent apoptosis-inducing effect of luteolin in two other cell lines, HepG2 and HAK-1B. By the luteolin treatment, both HepG2 cells and HAK-1B cells clearly showed cleavages in caspase-3 and PARP, accompanied by decrease in the expression level of Tyr⁷⁰⁵-phosphorylated STAT3 (Fig. 8A). Because HAK-1B cells were available for a xenograft

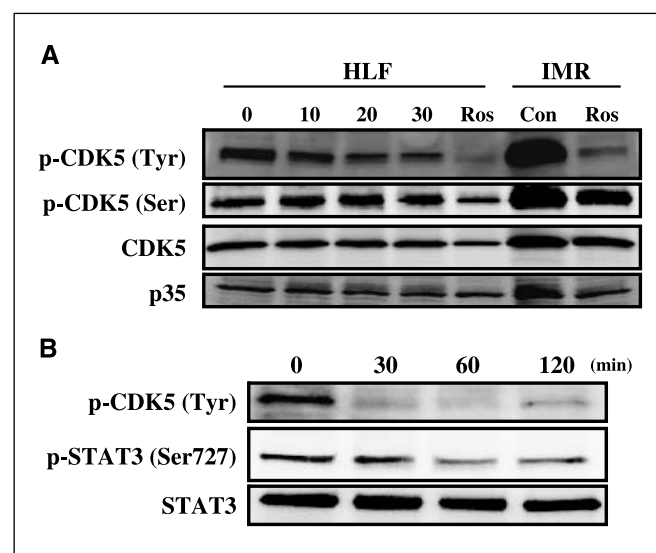
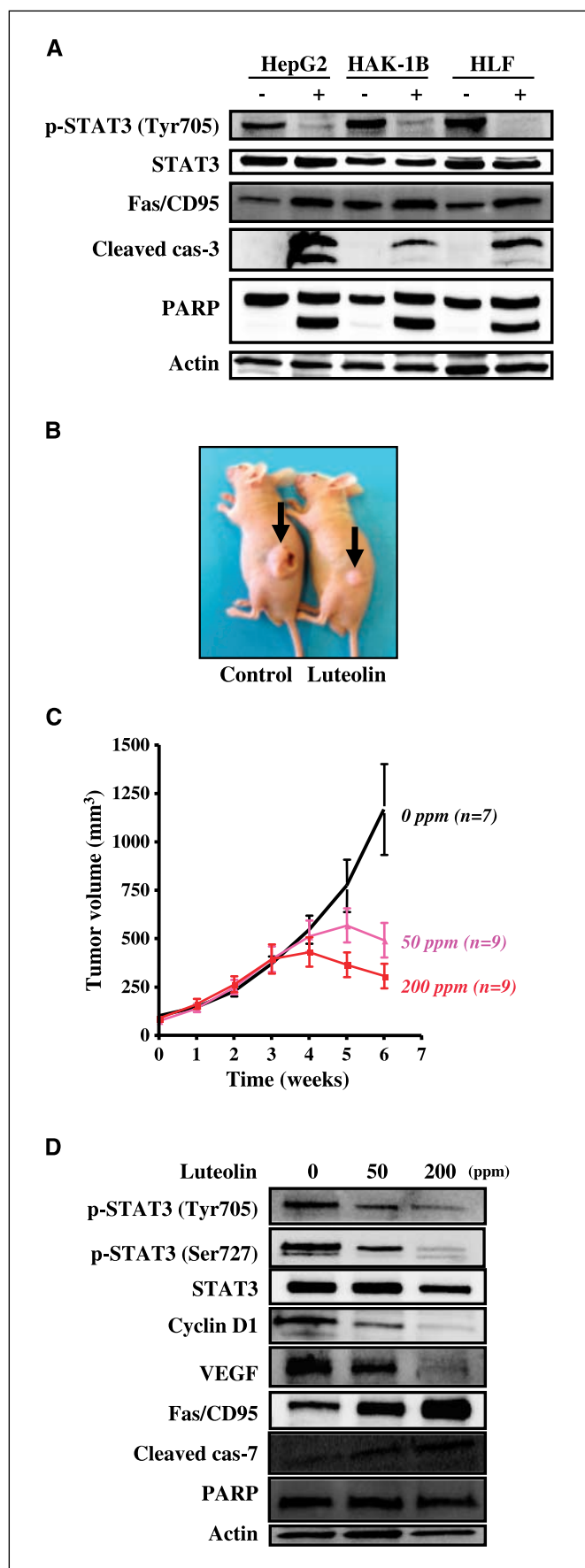


Figure 7. A, the hepatoma cells were incubated with 50 μmol/L luteolin for 0, 10, 20, and 30 minutes. A time-dependent decrease in the expression level of Tyr-phosphorylated CDK5 is noted in the immunoblot analyses. In contrast, the expression levels of Ser-phosphorylated CDK5 and p35 are unchanged by the luteolin treatments. The neuronal cell line IMR-32 (IMR) was set as the positive control for the active CDK5 expression. The expression levels of both Tyr-phosphorylated CDK5 and Ser-phosphorylated CDK5 are decreased by the CDK5 inhibitor, roscovitine (Ros, 10 μmol/L for 60 minutes incubation). B, a marked decrease in the expression level of Tyr-phosphorylated CDK5 is kept for at least 120 minutes by the 50 μmol/L luteolin treatment, followed by a gradual, but clear, decrease in that of Ser⁷²⁷-phosphorylated STAT3.



model in nude mice (27), the *in vivo* antitumor potential of luteolin was investigated (Fig. 8B). At 4 weeks after the beginning of luteolin-containing food intake, the HAK-1B tumor volume began to decrease in a dosage-dependent manner. After 5 weeks of the dietary luteolin treatment, a significant decrease in tumor volume was found even in mice taking 50 ppm luteolin-containing food (Fig. 8C). In concert with the decreased expressions in both Tyr⁷⁰⁵-phosphorylated STAT3 and Ser⁷²⁷-phosphorylated STAT3, a clear down-regulation in the target gene products of STAT3, such as cyclin D1 and VEGF, was found in the xenografted tumor tissues of the luteolin-treated mice, in a luteolin-dosage-dependent manner. Although an increased expression level of Fas/CD95 and a related cleavage in caspase-7 were confirmed in these tissue lysates, no clear cleavage was detected in PARP (Fig. 8D).

Discussion

In the present study, we have shown the following new findings: (a) luteolin increased the expression level of Fas/CD95 in neoplastic cells both *in vitro* and *in vivo*; (b) luteolin promoted the phosphorylation site-specific degradation in STAT3 through a ubiquitination-dependent process; and (c) luteolin significantly inhibited the growth in human hepatocellular carcinoma xenografts in nude mice.

Among several proposed mechanisms for the luteolin-induced apoptosis, the death receptor-associated mechanism has been recently receiving much attention. Shi et al. (10) first showed that luteolin sensitized TNF- α -induced apoptosis in malignant cells despite no significant increase in the TNFR1 expression level. Also, in our study, the expression level of TNFR1 was unchanged in the luteolin-treated hepatoma cells; however, a sensitization mechanism might underlie hepatoma cell apoptosis, presumably suppressing the expressions of the nuclear factor- κ B (NF- κ B)-targeted antiapoptotic genes (10). Very recently, it has been shown that luteolin up-regulated the death receptor 5 (DR5), thereby inducing apoptosis in human cancer cells and augmenting the apoptosis triggered by the DR5 ligand TNF-related apoptosis-inducing ligand (35, 36). These findings strongly suggested a critical involvement of the up-regulated death receptor superfamily-mediated signals in luteolin-induced cancer cell apoptosis. Also, in this study, up-regulation in another death receptor Fas/CD95 was first identified, even *in vivo*, in luteolin-treated human hepatoma cells, resulting in enhanced apoptosis via caspase-8 activation. It remains to be elucidated whether the death

Figure 8. A, a potent apoptosis-inducing effect of luteolin (50 μ mol/L) is shown in three hepatoma cell lines. A marked decrease in the expression level of Tyr⁷⁰⁵-phosphorylated STAT3 accompanied by an increase in the Fas/CD95 expression is confirmed in all three cell lines, resulting in clear cleavages of caspase-3 and PARP in immunoblot assay. B, inhibition in the size of the xenografted HAK-1B tumors (arrows) is shown in a representative mouse taking the luteolin (200 ppm)-containing food. C, a clear decrease in the volume of the xenografted tumors is found. A dosage-dependent antitumor potential of luteolin is found *in vivo*. D, the tissue lysates of xenograft tumors, containing 50 μ g protein each, were subjected to immunoblot analyses. The enhanced expression of Fas/CD95 is noted in the luteolin-exposed tumor lysates, in a dosage-dependent manner, in concert with the decreased expressions of both Tyr⁷⁰⁵-phosphorylated STAT3 and Ser⁷²⁷-phosphorylated STAT3. The decreased expressions are also shown in cyclin D1 and VEGF in a luteolin dosage-dependent manner. The cleavage of caspase-7 was found in the luteolin-exposed tumor lysates in a luteolin dosage-dependent manner; however, no clear cleavage was detected in PARP.

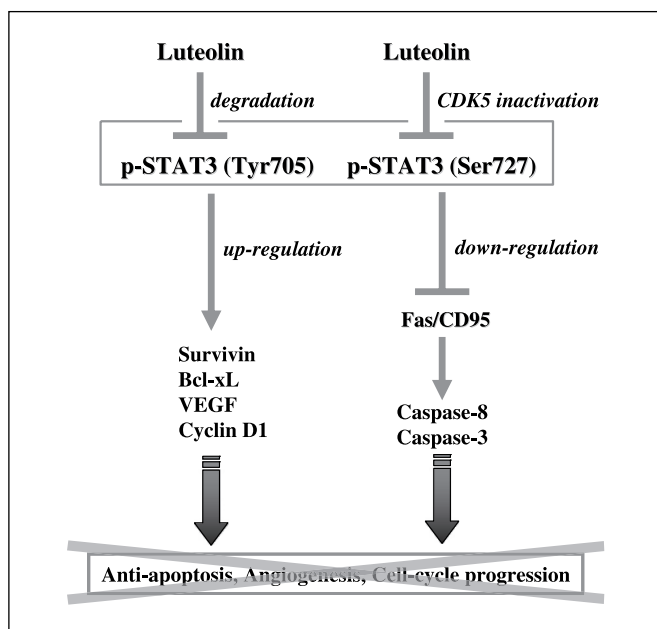


Figure 9. A schematic summary for the anticancer mechanisms of luteolin shown in the present study. Luteolin preferentially promotes the ubiquitin-dependent degradation in Tyr⁷⁰⁵-phosphorylated STAT3, and participates, at least in part, in the down-regulation of Ser⁷²⁷-phosphorylated STAT3 through inactivation of CDK5. This inactivation of STAT3 by luteolin may lead to the abrogation of the STAT3-mediated cancer properties, including antiapoptosis (survival), angiogenesis, and cell cycle progression, and increase sensitivity to apoptosis through up-regulation of Fas/CD95.

receptor-mediated apoptotic mechanism is ubiquitous in the flavonoid-induced apoptosis in malignant cells.

It has previously been shown that transcription of *Fas/CD95* was suppressed by the transcription factor, STAT3 (31). Because several up-regulated gene products by STAT3, such as cyclin D1, c-myc, Bcl-xL, survivin, and VEGF, are all critically involved in the development of cancer aggressiveness, targeting STAT3 is theoretically considered a fascinating anticancer strategy and has actually been shown to be valid in inducing a significant apoptosis in both the mice model of melanoma xenografts and that of squamous cell carcinoma xenografts (37, 38). Furthermore, ablation of STAT3 expression *in vivo* has provided a deep insight into a new candidate approach for the treatment of human lymphoma (39). In this context, our concerns converged in the potential effect of luteolin to down-regulate STAT3 expression as a putative mechanism for increased Fas/CD95 expression. Indeed, in this study, we found a drastic decrease in the expression level of Tyr⁷⁰⁵-phosphorylated STAT3, a major active form of STAT3. Consistent with this finding in immunoblotting assay, we confirmed the immediate disappearance in Tyr⁷⁰⁵-phosphorylated STAT3 from nuclei, where the activated STAT3 worked, in the luteolin-treated hepatoma cells by immunocytochemistry. If this striking down-regulation in active STAT3 is substantially responsible for the luteolin-induced apoptosis through augmenting Fas/CD95 expression, then enforced expression of STAT3 in hepatoma cells should result in luteolin resistance. Indeed, the transfected cells clearly expressed Tyr⁷⁰⁵-phosphorylated STAT3 despite exposure to cytotoxic concentrations of luteolin, resulting in less apoptosis. This finding strongly supports the concept that luteolin may induce apoptosis in human hepatoma cells by targeting the oncogenic transcription factor STAT3.

Although the precise mechanisms of STAT3 degradation have not yet been fully understood, it is evident that ubiquitination is involved in the proteasomal degradation of STAT3 (40–42). In the present study, we first showed an enhanced ubiquitination of Tyr⁷⁰⁵-phosphorylated STAT3 by the natural flavonoid luteolin. This novel effect by luteolin may provide insights into the antitumor properties of natural agents. Recently, a mumps virus-derived protein has been shown to be involved in ubiquitin-dependent degradation in STAT3 (42); however, it still remains unclear whether such degradation is dependent on the phosphorylation status of STAT3. It is well known that many target proteins (substrates) for degradation are recognized by the substrate-specific E3 ligase [termed the Skp1/Cull 1/F-box (SCF)] complex, resulting in proteasomal degradation (43). Several substrates are captured by their corresponding E3-ligase complexes in a substrate phosphorylation-dependent manner. For example, SCF^{Skp2} targets phosphorylated forms of p27^{Kip1} and p130. Thus, it is speculated that there may be a putative luteolin-(flavonoid)-responsive SCF machinery against Tyr⁷⁰⁵-phosphorylated STAT3 in a phosphorylation-dependent manner.

STAT3 confers tumorigenic advantages to neoplastic cells through up-regulating cyclin D1, Bcl-xL, survivin, and VEGF (15). In the present study, the expression levels in all of these downstream molecules of STAT3 were clearly down-regulated by luteolin not only *in vitro* but also *in vivo*, even in mice ingesting a low concentration (50 ppm) of luteolin. It was suggested that these down-regulations contributed to the potent growth inhibitory effect on the xenografted cancers. In contrast, the clear increase in the Fas/CD95 expression by the luteolin-induced down-regulation of STAT3 seemed to contribute less to the significant apoptosis of xenografted hepatoma cells *in vivo*. It was noteworthy that the expression level of Ser⁷²⁷-phosphorylated STAT3 was also clearly decreased. Because the Ser⁷²⁷ phosphorylation as well is known to regulate the transcriptional activity of STAT3 (20, 21), this attenuated phosphorylation was suggested to participate in the down-regulation of the transcriptional activity of STAT3 in the xenografted hepatoma cells in nude mice after long-term ingestion of luteolin. From our findings on the luteolin-induced dephosphorylation of CDK5, long-term exposure to luteolin *in vivo* might continuously inactivate CDK5, resulting in clear decrease in Ser⁷²⁷-phosphorylated STAT3 expression.

Although the actual anticancer effects by luteolin both *in vitro* and *in vivo* are not yet agreed upon, the findings from the present study have suggested a dual-pathway theory targeting STAT3; one is the promotion of ubiquitin-dependent degradation in Tyr⁷⁰⁵-phosphorylated STAT3 and the other is gradual down-regulation in Ser⁷²⁷-phosphorylated STAT3 through inactivation of CDK5. These events on phosphorylated STAT3s (Fig. 9) may trigger apoptosis in cancer cells, although minimally *in vivo*, and/or inhibit cancer-promoting properties via up-regulation in Fas/CD95 and down-regulations in cyclin D1, Bcl-xL, survivin, and VEGF.

Acknowledgments

Received 11/16/2005; revised 2/13/2006; accepted 3/7/2006.

Grant support: Project grant for establishing new high technology research centers and grant from the 21st Century Centers of Excellence Program for Medical Science from the Ministry of Education, Culture, Sports, Science, and Technology of Japan.

The costs of publication of this article were defrayed in part by the payment of page charges. This article must therefore be hereby marked *advertisement* in accordance with 18 U.S.C. Section 1734 solely to indicate this fact.

We thank Masako Shinkawa for technical assistance.

References

1. Ross JA, Kasum CM. Dietary flavonoids: bioavailability, metabolic effects, and safety. *Annu Rev Nutr* 2002; 22:19–34.
2. Ueda H, Yamazaki C, Yamazaki M. Inhibitory effect of *Perilla* leaf extract and luteolin on mouse skin tumor promotion. *Biol Pharm Bull* 2003;26:560–3.
3. Casagrande F, Darbon JM. Effects of structurally related flavonoids on cell cycle progression of human melanoma cells: regulation of cycle-dependent kinases CDK2 and CDK1. *Biochem Pharmacol* 2001;61: 1205–15.
4. Bagli E, Stefanidou M, Morbidelli L, et al. Luteolin inhibits vascular endothelial growth factor-induced angiogenesis: inhibition of endothelial cell survival and proliferation by targeting phosphatidylinositol 3'-kinase activity. *Cancer Res* 2004;64:7936–46.
5. Plaumann B, Fritsche M, Rimpler H, Brandner G, Hess RD. Flavonoids activate wild-type p53. *Oncogene* 1996; 13:1605–14.
6. Huang YT, Hwang JJ, Lee PP, et al. Effects of luteolin and quercetin, inhibitors of tyrosine kinase, on cell growth and metastasis-associated properties in A431 cells overexpressing epidermal growth factor receptor. *Br J Pharmacol* 1999;128:999–1010.
7. Lee L, Huang YT, Hwang JJ, et al. Blockade of the epidermal growth factor receptor tyrosine kinase activity by quercetin and luteolin leads to growth inhibition and apoptosis of pancreatic tumor cells. *Anticancer Res* 2002;22:1615–27.
8. Yamashita N, Kawanishi S. Distinct mechanisms of cDNA damage in apoptosis induced by quercetin and luteolin. *Free Radic Res* 2000;33:623–33.
9. Chowdhury AR, Sharma S, Mandal S, Goswami A, Mukhopadhyay S, Majumder HK. Luteolin, an abundant dietary component, is a potent anti-leishmanial agent that acts by inducing topoisomerase II-mediated kinetoplast DNA cleavage leading to apoptosis. *Biochem J* 2002;366:653–61.
10. Shi RX, Ong CN, Shen HM. Luteolin sensitizes tumor necrosis factor- α -induced apoptosis in human tumor cells. *Oncogene* 2004;23:7712–21.
11. Cheng AC, Huang TC, Lai CS, Pan MH. Induction of apoptosis by luteolin through cleavage of Bcl-2 family in human leukemia HL-60 cells. *Eur J Pharmacol* 2005;509: 1–10.
12. Lee HJ, Wang CJ, Kuo HC, Chou FP, Jean LF, Tseng TH. Induction of apoptosis of luteolin in human hepatoma HepG2 cells involving mitochondria translocation of Bax/Bak and activation of JNK. *Toxicol Appl Pharmacol* 2005;203:24–31.
13. Chang J, Hsu Y, Kuo P, Kuo Y, Chiang L, Lin C. Increase of Bax/Bcl-XL ratio and arrest of cell cycle by luteolin in immortalized human hepatoma cell line. *Life Sci* 2005;76:1883–93.
14. Brusselmans K, Vrolix R, Verhoeven G, Swinnen JV. Induction of cancer cell apoptosis by flavonoids is associated with their ability to inhibit fatty acid synthase activity. *J Biol Chem* 2005;280:5636–45.
15. Yu H, Jove R. The STATs of cancer—new molecular targets come of age. *Nat Rev Cancer* 2004;4:97–105.
16. Garcia R, Jove R. Activation of STAT transcription factors in oncogenic tyrosine kinase signaling. *J Biomed Sci* 1998;5:79–85.
17. Catlett-Falcone R, Landowski TH, Oshiro MM, et al. Constitutive activation of Stat3 signaling confers resistance to apoptosis in human U266 myeloma cells. *Immunity* 1999;10:105–15.
18. Bromberg JF, Wrzeszczynska MH, Devgan G, et al. Stat3 as an oncogene. *Cell* 1999;98:295–303.
19. Darnell JE, Jr., Kerr IM, Stark GR. Jak-STAT pathways and transcriptional activation in response to IFNs and other extracellular signaling proteins. *Science* 1994;264: 1415–21.
20. Wen Z, Zhong Z, Darnell JE, Jr. Maximal activation of transcription by Stat1 and Stat3 requires both tyrosine and serine phosphorylation. *Cell* 1995;82:241–50.
21. Yokogami K, Wakisaka S, Avruch J, Reeves SA. Serine phosphorylation and maximal activation of STAT3 during CNTF signaling is mediated by the rapamycin target mTOR. *Curr Biol* 2000;10:47–50.
22. Darnell JE. Validating Stat3 in cancer therapy. *Nat Med* 2005;11:595–6.
23. Mapelli M, Musacchio A. The structural perspective on CDK5. *Neurosignals* 2003;12:164–72.
24. Chen F, Wang Q, Wang X, Studzinski GP. Up-regulation of Egr1 by 1,25-dihydroxyvitamin D3 contributes to increased expression of p35 activator of cyclin-dependent kinase 5 and consequent onset of the terminal phase of HL60 cell differentiation. *Cancer Res* 2004;64:5425–33.
25. Fu AK, Fu WY, Ng AK, et al. Cyclin-dependent kinase 5 phosphorylates signal transducer and activator of transcription 3 and regulates its transcriptional activity. *Proc Natl Acad Sci U S A* 2004;101:6728–33.
26. Yano H, Iemura A, Fukuda K, Mizoguchi A, Haramaki M, Kojiro M. Establishment of two distinct human hepatocellular carcinoma cell lines from a single nodule showing clonal dedifferentiation of cancer cells. *Hepatology* 1993;18:320–7.
27. Hisaka T, Yano H, Ogasawara S, et al. Interferon- α Con1 suppresses proliferation of liver cancer cell lines *in vitro* and *in vivo*. *J Hepatol* 2004;41:782–9.
28. Koga H, Sakisaka S, Harada M, et al. Involvement of p21^{WAF1/Cip1}, p27^{Kip1}, and p18^{INK4c} in troglitazone-induced cell-cycle arrest in human hepatoma cell lines. *Hepatology* 2001;33:1087–97.
29. Yoshida T, Hanada T, Tokuhisa T, et al. Activation of STAT3 by the hepatitis C virus core protein leads to cellular transformation. *J Exp Med* 2002;196:641–53.
30. Koga H, Harada M, Ohtsubo M, et al. Troglitazone induces p27^{Kip1}-associated cell cycle arrest through down-regulating Skp2 in human hepatoma cells. *Hepatology* 2003;37:1086–96.
31. Ivanov VN, Bhoumik A, Krasilnikov M, et al. Cooperation between STAT3 and c-jun suppresses Fas transcription. *Mol Cell* 2001;7:517–28.
32. Hershko A. Roles of ubiquitin-mediated proteolysis in cell cycle control. *Curr Opin Cell Biol* 1997;9:788–99.
33. Nakayama KI, Hatakeyama S, Nakayama K. Regulation of the cell cycle at the G₁-S transition by proteolysis of cyclin E and p27^{Kip1}. *Biochem Biophys Res Commun* 2001;282:853–60.
34. Strocchi P, Pession A, Dozza B. Up-regulation of CDK5/p35 by oxidative stress in human neuroblastoma IMR-32 cells. *J Cell Biochem* 2003;88:758–65.
35. Horinaka M, Yoshida T, Shiraishi T, et al. Luteolin induces apoptosis via death receptor 5 upregulation in human malignant tumor cells. *Oncogene* 2005;24: 7180–9.
36. Horinaka M, Yoshida T, Shiraishi T, et al. The combination of TRAIL and luteolin enhances apoptosis in human cervical cancer HeLa cells. *Biochem Biophys Res Commun* 2005;333:833–8.
37. Niu G, Heller R, Catlett-Falcone R, et al. Gene therapy with dominant-negative Stat3 suppresses growth of the murine melanoma B16 tumor *in vivo*. *Cancer Res* 1999; 59:5059–63.
38. Xi S, Gooding WE, Grandis JR. *In vivo* antitumor efficacy of STAT3 blockade using a transcription factor decoy approach: implications for cancer therapy. *Oncogene* 2005;24:970–9.
39. Chiarle R, Simmons WJ, Cai H, et al. Stat3 is required for ALK-mediated lymphomagenesis and provides a possible therapeutic target. *Nat Med* 2005;11: 623–9.
40. Daino H, Matsumura I, Takada K, et al. Induction of apoptosis by extracellular ubiquitin in human hematopoietic cells: possible involvement of STAT3 degradation by proteasome pathway in interleukin 6-dependent hematopoietic cells. *Blood* 2000;95:2577–85.
41. Perry E, Tsruya R, Levitsky P, et al. TMF/ARA160 is a BC-box-containing protein that mediates the degradation of Stat3. *Oncogene* 2004;23:8908–19.
42. Ulane CM, Kentsis A, Cruz CD, Parisien JP, Schneider KL, Horvath CM. Composition and assembly of STAT-targeting ubiquitin ligase complexes: paramyxovirus V protein carboxyl terminus is an oligomerization domain. *J Virol* 2005;77:6385–93.
43. Pagano M. Control of DNA synthesis and mitosis by the Skp2-p27-Cdk1/2 axis. *Mol Cell* 2004;14:414–6.